

## THE WARPED DISK OF INTEGRAL-SIGN GALAXY PGC 20348

H. B. ANN

Division of Science Education, Pusan National University, Busan 609-735, Korea

*E-mail: hbann@pusan.ac.kr*

*(Received January 18, 2007; Accepted March 6, 2007)*

### ABSTRACT

We examine the morphology and luminosity distribution of a strongly warped spiral galaxy PGC 20348 by conducting a detailed *BVI* CCD surface photometry using BOAO 1.8m telescope. The radial surface brightness shows a break at warp radius ( $r_w$ ) with a shallow gradient in the inner disk and a steeper gradient in the outer disk. The luminosity of east side of the disk is  $\sim 0.5$  mag fainter than the west side at  $r > r_w$ . The reason for the asymmetric luminosity distribution is thought to be the asymmetric flarings that result in the formation of a large diffuse region at the edge of the east disk and a smaller diffuse region at the west disk. The vertical luminosity profiles show a thick disk component whose scale heights increase with increasing galactocentric distances. The warp of PGC 20348 seems to be made by the tidal interactions with the two massive companion galaxies since the flarings and radial increase of disk scale heights are thought to be general properties of tidally perturbed disks. According to the colors of the two clumps inside the diffuse region at the edge of the east disk, they seem to be sites of active star formation triggered by tidal forces from the companion galaxies.

*Key words* : galaxies:individual — galaxies:evolution — galaxies:disk — galaxies:structure — method — CCD photometry

### I. INTRODUCTION

More than half of the spiral galaxies have warped disks (Sanchez-Saavedra et al. 1990; Reshetnikov & Combes 1998; Ann & Park 2006). Radio warps are usually more conspicuous than optical warps (Sancisi 1976; Bosma 1981) but some of stellar disks are also highly warped. The warp of PGC 20348 whose morphology resembles an integral sign is one of the best examples of strong optical warps. The morphology of the warp of PGC 20348 is a characteristics of S-shaped warps which are more frequently observed than U-shaped warps (Reshetnikov & Combes 1998; Ann & Park 2006).

Many mechanisms have been proposed to explain the origin of warps (see review by Binney 1992). Among the proposed mechanisms, tidal disturbances by nearby galaxies and gravitational torques from misaligned halos (Debattista & Sellwood 1999; Ideta et al. 2000) are thought to be dominant mechanisms for interacting galaxies and isolated galaxies, respectively. However, accretion of the intergalactic medium (Ostriker & Binney 1989; Jiang & Binney 1999; Lopez-corredoria et al. 2002) and bending instability of self-gravitating disks (Sparke 1995; Revaz & Pfenniger 2004) may also play significant role for driving and maintenance of warps.

Owing to recent warp statistics in spiral galaxies by Ann & Park (2006), it is quite apparent that warps are ubiquitous in spiral galaxies with variety of strength and morphology. However, detailed investigations of warped disks for individual galaxies are quite rare. Since strong warps are thought to be caused by the tidal forces from the companion galaxies (Reshetnikov

& Combes 1998; Garcia-Ruiz, Sancisi, & Kuijken 2002; Ann & Park 2006), it seems quite plausible that the vertical structure of the strongly warped disks is much different from that of the weakly warped or non-warped disks due to the different external tidal heating. In extreme cases, the strong tidal force may detach some disk stars from the outer disks.

The behavior of disk scale height along the galactocentric distance is closely related to the formation and evolution of the galactic disks. Earlier investigations of the vertical profiles of edge-on galaxies showed that they are constant over the whole disk (van der Kruit & Searle 1981a, b; Waincoat, Freeman & Hyland 1989; Shaw & Gilmore 1990; Barnaby & Thronson 1992). The constant disk scale height over the galactic disk is consistent with the theoretical picture of secular disk heating by massive molecular clouds (Spitzer & Schwarzschild 1951; Binney 1981). However, there are a number of galaxies that display significant variations of disk scale heights (de Grijs & van der Kruit 1966; Reshetnikov & Combes 1996, 1997). In particular, interacting/merging galaxies tend to have increasing disk scale height with increasing galactocentric distance (Schwarzkopf & Dettmar 2001). Moreover, there are some galaxies showing similar behavior of disk scale height in non-interacting galaxies (de Grijs & Peletier 1997). Thus, it seems likely that there are many mechanisms that control the behavior of disk scale heights. The accretion of small companions (Töth & Ostriker 1992; Quinn et al 1993; Walker et al. 1996) is a viable scenario for the systematic variation of disk scale heights in galaxies with and without interactions.

PGC 20348 is a late type spiral galaxy (Sd) which has two companions of comparable masses (PGC 20362 and PGC 20398). One interesting feature displayed by deep photographic plates is the diffuse region near the south-east edge of the warped disk. Since it is too faint to be analyzed in detail, Ann & Park (2006) neglected it in their analysis of the warp properties. However, it seems plausible that it is a flared disk material caused by the tidal forces of the two massive companions or a tidal debris of recently merged satellite. Because the diffuse region is likely to be made by the same mechanism that drives the strong warp of PGC 20348, a detailed analysis of the warped disk including the diffuse regions may provide some clues to understand the mechanism that generate strong warps.

The primary aim of the present study is to analyze the vertical structure of the disk of PGC 20348 which is believed to be affected by the warping forces that generate the strong S-shaped warp. Since the vertical structure of the disk is closely related to the warp properties, a close examination of vertical structure, based on a detailed surface photometry, will lead to better understanding of the warped disk. To do this, we conducted a deep *BVI* CCD surface photometry of PGC 20348. In §2, we describe the observations and the data reduction and the results are presented in §3. Summary and discussion are given in the final section.

## II. OBSERVATIONS

### (a) Observations and Basic Reduction

We obtained deep CCD images of PGC 20348 using SITE 2048 × 2048 CCD with Johnson-Cousins *BVI* filters attached to the F/8 cassegrain focus of the BOAO 1.8m telescope. The pixel size of the CCD is 24 μm, which yields the field of view of 11.7′ × 11.7′. The gain and readout noise of the CCD are 1.8 electrons/ADU and 7 electrons, respectively. We observed several Landolt (1992) stars for calibration of the photometry. Table 1 presents the log of observations.

We followed the standard procedure of CCD reductions using IRAF/CCDRED to obtain flat-fielded images. This includes the subtraction of bias, overscan correction, trimming, and flat-fielding. The correction of dark current was not applied because it is negligible. For stellar photometry of standard stars we used the IRAF/APPHOT to derive the instrumental magnitudes.

### (b) Surface Photometry

We conducted a surface photometry of PGC 20348 using SPIRAL (Ichikawa et al. 1987) which allows the subtraction of sky background, smoothing, and cleaning of the foreground stars. Since warps are usually found in the faint outer disks, it is essential to subtract the sky background as accurate as possible. To do this,

TABLE 1.  
JOURNAL OF OBSERVATIONS

| FILTER | T <sub>exp</sub> | SEEING | DATE          |
|--------|------------------|--------|---------------|
| B      | 900s × 2         | 1."8   | JAN. 24, 2004 |
| V      | 900s × 3         | 2."0   | JAN. 24, 2004 |
| I      | 300s × 3         | 1."6   | JAN. 24, 2004 |

we applied a two-dimensional polynomial of

$$S(x, y) = a_0 + a_1x + a_2y$$

to the regions surrounding the target galaxies where  $S$  is sky intensity. The sky subtracted images were smoothed by Gaussian filters to reduce noises that make the isophotes of the outer disk too irregular. The smoothed images were used for the analysis of the vertical structure of disk as well as the warp parameters.

The calibration of the present photometry was made by determining the sky surface brightness because the surface brightness of galaxy is expressed as

$$\mu(x, y) = \mu_{sky}(x, y) - 2.5 \log G(x, y)$$

where  $G(x, y)$  is expressed in unit of sky intensity  $S(x, y)$ . We determined the zero point and extinction coefficients from the aperture photometry of the standard stars observed during the observing night. However, we used the mean color coefficients derived from the standard stars observed during the observing run to transform the instrumental magnitudes to the standard system.

## III. RESULTS

### (a) Morphology

Fig. 1 shows the *B*-band grey-scale images of PGC 20348 demonstrating the S-shaped warp resembling an integral-sign. As shown in the top image which better displays the bright part of the galaxy, the warped disk of PGC 20348 is highly asymmetric, i.e., larger warp amplitude in the west side of the disk. However, if we consider the diffuse flarings as parts of the warps (see the bottom image of Fig. 1), the warp asymmetry is much reduced because the flaring in the east-side disk is more extended than that of the west-side disk. There is no significant morphological differences among images observed in different pass-bands (Fig. 2). However, the dust extinction is much reduced in the *I*-band image.

It is difficult to identify the nucleus of PGC 20348 due to the negligible bulge. There are a number of clumps along the disk major axis. The majority of the clumps are HII region complexes obscured by dust but the largest clump located near  $r \sim 25''$  east (indicated as C in Fig. 1) is thought to be a remnant of merged satellite since it is much larger, brighter, and bluer than

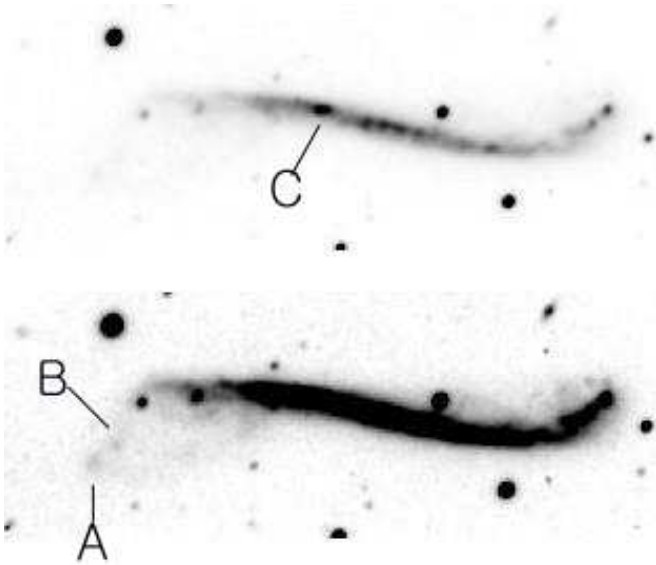


**Fig. 1.**— The  $B$ -band gray scale images of PGC 20348. Display level was adjusted to show the bright parts of the disk in the top image and the outer disk in the bottom image, respectively. The symbols 'A' and 'B' denote the blue clumps in the diffuse region and 'C' indicates the largest clump at  $r \approx 25''$  east in the top image. North is in the top and east is to the left.

any other clumps. It is even brighter than the nucleus. The colors of the largest clumps are  $B - V = 0.54$  and  $V - I = 0.78$  whereas the three clumps in the nuclear regions of which the central one is the nucleus have redder colors of  $B - V = 0.83 \sim 0.90$  and  $V - I = 1.11 \sim 1.28$ .

The morphology and locations of the diffuse regions imply that they are consisted of disk material detached from the warped disk. However, there is a possibility that some parts of the diffuse regions, especially some regions far from the disk, are tidal debris of disrupted satellite. There are some clumps inside the diffuse regions. The bright round source close to the east edge of the disk seems to be a foreground star but the two clumps denoted as A and B in Fig. 1, are thought to be sites of active star formation since they are bluer than the surrounding regions. The clump A and clump B have the colors of  $B - V = 0.60$ ,  $V - I = 0.67$  and  $B - V = 0.61$ ,  $V - I = 0.48$ , respectively.

### (b) Warp Parameters

The properties of warps can be characterized by three warp parameters, warp radius, warp amplitude, and warp asymmetry. Warp radius  $r_w$  is defined by the radius where the disk begins to bend away from the middle plane of the disk. Warp amplitude, which is closely related to the strength of warping force, is usually defined by warp angles. Most commonly used

TABLE 2.  
WARP PARAMETERS

| $r_w$     | $\alpha_e$    | $\alpha_w$    | $\beta_e$  | $\beta_w$  | $A_\alpha$   |
|-----------|---------------|---------------|------------|------------|--------------|
| $13.3kpc$ | $21.^\circ 8$ | $16.^\circ 7$ | $35^\circ$ | $31^\circ$ | $5.^\circ 1$ |

warp angle is the warp angle  $\alpha$  which is defined by the angle between the mean major axis of the inner disk and the line connecting the center of the galaxy and the tips of the outermost isophotes. The warp angle measured in the east side of the disk is  $\alpha_e$  and that of the west side of the disk is  $\alpha_w$ . There is another warp angle  $\beta$  which is defined by the line connecting the position of  $r = r_w$  and the tips of the outermost isophotes. The warp angle  $\beta$  seems to better represent the curvature of the warped disk (Ann & Park 2006). There are different definitions of warp asymmetry in the literature (Reshetnikov & Combes 1998; Garcia-Ruzi et al. 2002; Castro-Rodriguez et al. 2002) but we used the following definition of  $A_\alpha = |\alpha_e - \alpha_w|$ .

We determined the warp angles ( $\alpha$  and  $\beta$ ) and the warp radius using the  $B$ -band isophotal maps shown in Fig. 2. The warp parameters derived from the  $V$  and  $I$ -band isophotal maps are nearly the same as those from  $B$ -band. We considered the flarings in either side of the disk as parts of warps in measuring the warp parameters. We listed the warp parameters in Table 2. We used the distance of PGC 20348 as 41.8 Mpc that is derived from its radial velocity in NED using  $H = 75km/s/Mpc$ . The present estimate of  $\alpha_e$  is about two times larger than that of Ann & Park (2006) while  $\alpha_w$  is almost the same. Thus, there is no significant asymmetry in warp amplitude. The reason for the discrepancy between the present measure of  $\alpha_e$  and that of Ann & Park (2006) is due to the different level of the surface brightness of the outermost isophotes. The present photometry reveals the faint outer disk  $\sim 5$  mag below the sky surface brightness, which allows an easy identification of the flarings, while the images from the photographic plates (Ann & Park 2006) hardly display the flarings.

### (c) Radial Profiles

In Fig. 3, we present three luminosity profiles along the major axis in  $B$ -band. The short-dashed line and dotted line represent the luminosity profiles extracted along the major axis of the east and west side of the disk, respectively, while the solid line indicates the major axis profile derived from an ellipse fitting. The luminosity profiles along the major axis that are measured by an aperture photometry reflect the clumpiness of the luminosity distribution along the disk major axis, especially in the west side of the disk. The noisy pattern of the luminosity profiles at  $r \lesssim 20''$  is due to the presence of bright clumps and dust lanes. The large bump near  $r \approx 25''$  in the elliptically averaged profile and the

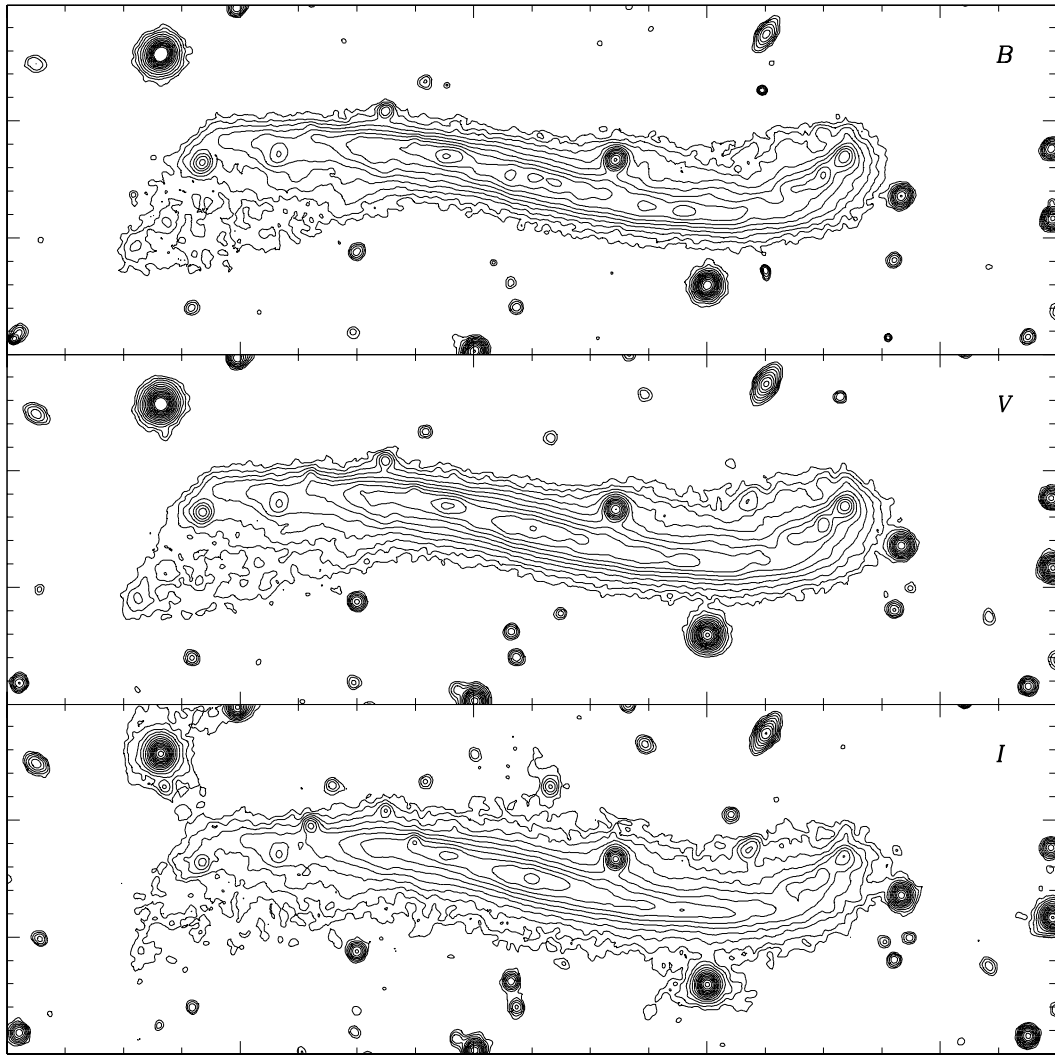


**Fig. 2.**— The *BVI* isophotal maps of PGC 20348. The outermost isophotes are 4 mag, 4.5 mag and 5 mag below sky brightness for *B*, *V*, and *I* bands, respectively.

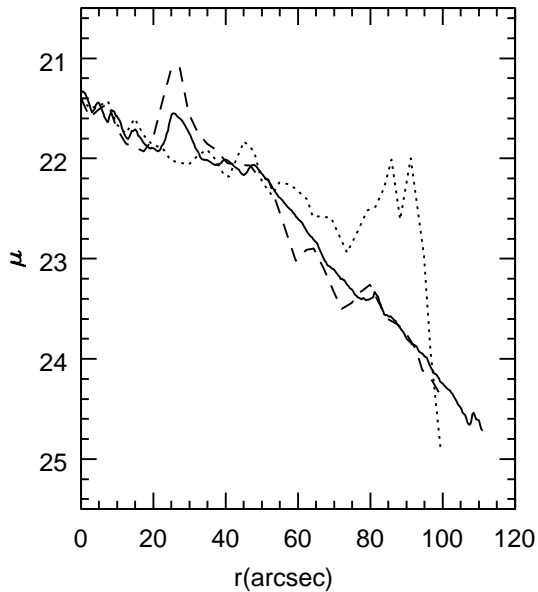


**Fig. 3.**— Radial profiles of PGC 20348. The solid line represents the elliptically averaged profile, while the short-dashed and dotted lines indicate the major axis profile extracted at the east and west side of the disk, respectively.

east-side profile is caused by the largest clump which is thought to be a remnant of merged satellite. As is clearly seen in the luminosity profile of the east side of the disk (short-dashed line in Fig. 3), the luminosity of this clump is brighter than that of the nucleus. The large bump at  $r \approx 90''$  in the west-side profile, which shows two peaks, is caused by foreground stars.

There are two interesting features in the radial profiles. Firstly, there is an abrupt change of luminosity gradient at  $r = r_w$  where the disk of PGC 20348 begins to bend away from the middle plane of the disk. The luminosity distribution at  $r < r_w$  shows a shallow gradient that resembles the luminosity distribution of the strongly barred galaxies in the barred regions, while the luminosity distribution at  $r > r_w$  shows a very steep gradient. Secondly, the luminosity of the east disk is nearly the same as that of the west disk at  $r < r_w$ , i.e.,  $r < 50''$ , where as the luminosity of the east disk is somewhat fainter than that of the west disk at  $r > r_w$ , if we take into account the effects of clumps and dust lanes. The fainter luminosity of the east disk is due to its steeper gradient than that of the west disk. The reason for the asymmetric luminosity distribution is not apparent but it seems to be related to the asymmetric diffuse regions at the edges of the either side of the disk, if the diffuse regions are disk materials torn off during the tidal interactions that make the unusually strong warp of PGC 20348. It seems likely that more disk material is torn off in the east side of the disk to make its luminosity fainter than the west disk.

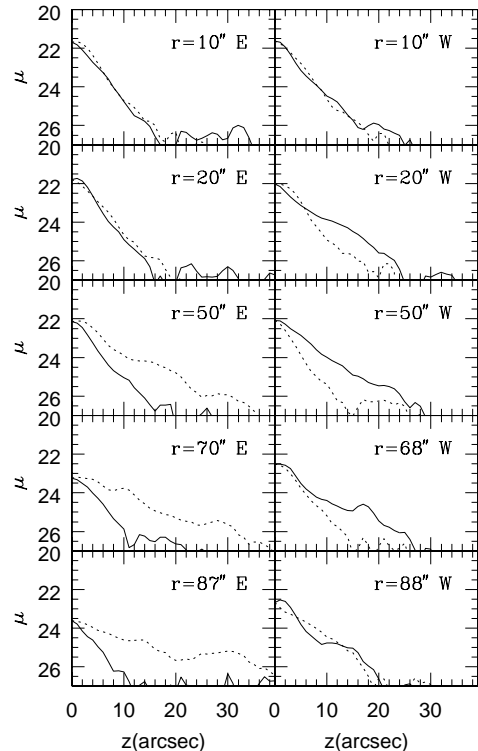


**Fig. 4.**— Vertical profiles extracted at 10 positions along the major axis of the disk. The solid lines represent the vertical profiles in the upper parts of the disk, while the dotted lines indicate those of the lower part of the disk.

#### (d) Vertical Profiles

Fig. 4 shows  $B$ -band vertical profiles which are extracted along the lines perpendicular to the disk major axis at 10 positions. The solid lines represent the vertical luminosity distribution of the upper part of the disk (upper profiles) and the dotted lines indicate those of the lower part of the disk (lower profiles). In central regions ( $r \lesssim 20''$ ), the upper and lower vertical profiles extracted at the same radii are very similar and well represented by a single exponential function. The large discrepancy between the upper profile and the lower profile in the west side of the disk at  $r = 20''$  is caused by a bright foreground star. In the outer parts of the disk ( $r > 50''$ ), lower profiles have shallower gradient than the upper profiles in the east side of disk, while the lower profiles have steeper gradient than the upper ones in the west side. The shallow gradients in the vertical profiles of the outer disk are due to the diffuse regions in the concave sides of the warp (see Fig. 2). Thus, the disk scale heights can be better derived from the vertical profiles in the convex sides of warp because they are less affected by the warp.

There seems to be a thick disk component in PGC 20348. The signature of the thick disk is the slight changes of luminosity gradient at  $z \approx 6''$  in the vertical

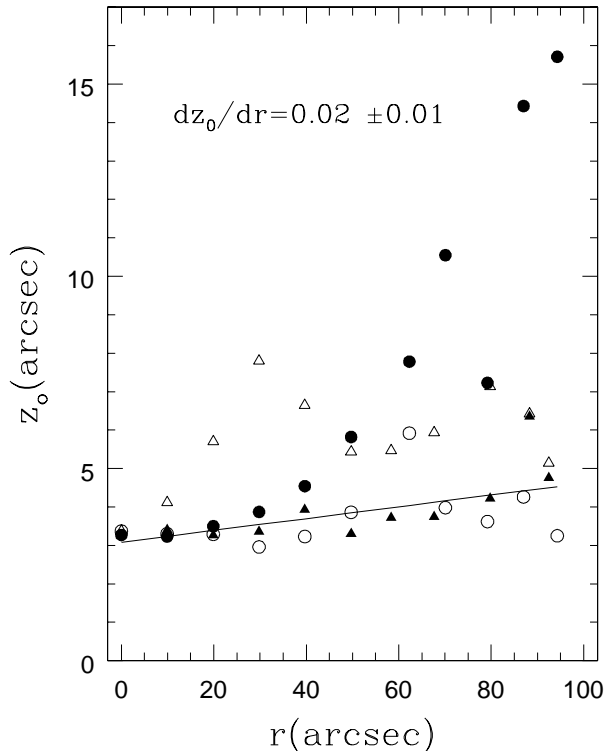


**Fig. 5.**— Disk scale heights as a function of galactocentric distance. The scale heights derived from the east side of the disk are plotted as circles, while those of the west side of the disk are plotted as triangles. The solid symbols are from the upper vertical profiles and the open symbols are from the lower vertical profiles, respectively

profiles extracted at  $r = 20''$  and  $r = 50''$ . Moreover, if we consider the diffuse regions that make the shallow gradients in the vertical profiles are made of disk materials detached by tidal interactions, PGC 20348 has an extremely large thick disk.

Fig. 5 shows the distributions of disk scale heights,  $z_o$  as a function of galactocentric distance. We fitted a single exponential functions to the vertical profiles at  $z = 3'' \sim 14''$  to derive  $z_o$  although some of the vertical profiles have multiple slopes due to thick disk component. The fitting range was selected by considering the extent of the vertical structure inferred from Fig. 3. As shown in Fig. 5, the disk scale heights derived from the less perturbed parts of the disk, i.e., the upper profiles in the east disk and the lower profiles in the west disk increase very slowly with galactocentric distance, while those derived from the heavily perturbed disk, i.e., the lower profiles in the east disk increase rapidly after  $r \approx 40''$ . The scale heights of the perturbed disk in the west side also increase with galactocentric distance even though there are large scatters due to foreground objects. The solid line in Fig.5 represents the mean relation between the disk scale height  $z_o$  and galactocentric distance, derived from the less perturbed parts of

the disk. As shown in Fig.5, the radial gradient of disk scale height  $dz_o/dr$  is very small,  $dz_o/dr = 0.02 \pm 0.01$ . The positive radial gradient is consistent with the general behavior of disk scale heights for warped disks (Schwarzkopf & Dettmar 2001).

#### IV. SUMMARY AND DISCUSSION

We have analyzed the luminosity distribution and warp parameters by conducting a detailed *BVI* CCD surface photometry. Our photometry was deep enough to reveal the detailed morphology of the outer disk of PGC 20348 which is  $\sim 5$  mag fainter than the local sky brightness. The present estimates of the warp parameters are essentially the same as those of Ann & Park (2006) but the warp angles of the east side of the disk,  $\alpha_e$  and  $\beta_e$  are larger than those of Ann & Park (2006) due to the diffuse region that is thought to be disk material detached by tidal forces of companion galaxies. We considered it as a part of warped disk while Ann & Park (2006) neglected it because their photographic images did not show the diffuse region as apparent as in the present CCD images. There are diffuse regions around the north-west edge of the disk too, but they do not significantly affect the warp angles since they are much smaller than the diffuse region near the south-east edge of the disk.

The luminosity distribution along the major axis of the disk shows an abrupt break in the luminosity gradient near the warp radius ( $r_w$ ) where the disk begins to bend away from the disk middle plane. The surface brightness of the inner disk ( $r < r_w$ ) shows a shallow gradient while that of the outer disk shows a steep gradient with steeper gradient in the east disk. The luminosity of the east disk is  $\sim 0.5$  mag fainter than that of the west disk at  $r > r_w$  due to more rapid decline of the surface brightness in the east disk. The fainter east disk beyond the warp radius is thought to be caused by the flarings during strong tidal interactions that make the diffuse region near the east edge of the disk.

The vertical profiles extracted at various positions along the major axis of the disk reveal a thick disk component which has shallower vertical luminosity gradient than the thin disk (Burstein 1979; van de Kruit & Searle 1981a, b). The existence of a thick disk is more apparent in the concave sides of the warped disk than the convex sides. This means that the vertical profiles are asymmetric with respect to the disk middle plane, especially in the outer disk ( $r > r_w$ ) due to the diffuse regions in the concave sides of the warped disk. Since the extremely strong warp of PGC 20348 is caused by the tidal forces of massive companions, the diffuse regions in the concave sides of the warped disk are thought to be the results of flarings driven by the tidal interactions.

There is a radial increase of disk scale height (i.e.,  $dz_o/dr > 0$ ) in PGC 20348. The extremely large disk scale height near the edge of the east disk is due to the large diffuse region that is almost detached from

the main disk. Similar flarings and radial increase of disk scale heights were observed in VV 490 that has a close companion (Reshetnikov & Combes 1996, 1997). Such a radial increase of disk scale heights is a general property of tidally perturbed disks (Schwarzkopf & Dettmar 2001) which can be explained by the tidal heating by companions or merged satellites (Töth & Ostriker 1992; Mihos et al. 1995).

There seem to be young stellar populations in the diffuse region near the east edge of the disk. The colors of the two clumps, indicated as A and B in Fig. 1, are much bluer than the surrounding regions. Since young stellar populations are frequently observed in the outer regions of strongly warped disks (Ann & Lee 2007), they are thought to be sites of active star formation triggered by the tidal forces from companion galaxies. However, the largest clump (C in Fig. 1) that also has blue colors is thought to be a remnant of merged satellite since it is too large and bright to be considered as HII regions in the disk of PGC 20348.

#### ACKNOWLEDGEMENTS

This work was supported for two years by Pusan National University Research Grant.

#### REFERENCES

- Ann, H. B. & Park, J.-C., 2006, Warped disks in spiral galaxies, *New Astronomy*, 11, 293
- Ann, H. B. & Lee, K. M., 2007, in preparation.
- Barnaby, D. & Thronson, H. A. Jr., 1992, The distribution of light in galaxies - The edge-on spiral NGC 5907, *AJ*, 103, 41
- Binney, J., 1981, Resonant excitation of motion perpendicular to galactic planes, *MNRAS*, 196, 455
- Binney, J., 1992, Warps, *ARA&A*, 30, 51
- Burstein, D., 1979, Structure and origin of S0 galaxies. III - The luminosity distribution perpendicular to the plane of the disks in S0's, *ApJ*, 234, 829
- Bosma, A., 1981, 21-cm line studies of spiral galaxies. I - Observations of the galaxies NGC 5033, 3198, 5055, 2841, and 7331. II - The distribution and kinematics of neutral hydrogen in spiral galaxies of various morphological types, *AJ*, 86, 1791
- Castro-Rodriguez, N., Lopez-Corredoira, M., Sanchez-Saavedra, M. L., & Battaner, E., 2002, Warps and correlations with intrinsic parameters of galaxies in the visible and radio, *A&A*, 391, 519
- Debattista, V. P. & Sellwood, J. A. 1999, Warped galaxies from misaligned angular momenta, *ApJ*, 513, L107
- Garcia-Ruiz, I., Sancisi, R., & Kuijken, K., 2002, Neutral hydrogen and optical observations of edge-on galaxies: Hunting for warps, *A&A*, 394, 769
- de Grijs, R. & Peletier, R. F., 1997, The shape of galaxy disks: how the scale height increases with galactocentric distance, *ã320*, L21
- de Grijs, R. & van der Kruit, P. C., 1996, Structure analysis of edge-on spiral galaxies, *A&AS*, 117, 19
- Ichikawa, S.-I., Okamura, S., Watanabe, M., Hamabe, M., Aoki, T., & Kodaira, K., 1987, SPIRAL : surface photometry interactive reduction and analysis library, *Ann. Tokyo Astro. Obs.* 21, 285
- Ideta, M., Hozumi, S., Tsuchiya, T., & Takizawa, M., 2000, Time evolution of galactic warps in prolate halos, *MNRAS*, 311, 733
- Jiang, I. & Binney, J., 1999, Warps and cosmic infall, *MNRAS*, 303, L7
- Landolt, A. U., 1992, UBVRI photometric standard stars in the magnitude range 11.5-16.0 around the celestial equator, *AJ*, 104, 340
- Lopez-Corredoira, M., Betancort-Rijo, J., & Beckman, J. E., 2002, Generation of galactic disc warps due to intergalactic accretion flows onto the disc, *A&A*, 386, 169
- Mihos, J. C, Walker, I. R., Hernquist, L., Mendes de Oliveira, C., & Bolte, M., 1995, A Merger origin for X Structures in S0 galaxies, *ApJ*, 447, L87
- Ostriker, E. C. & Binney, J., 1989, Warped and tilted galactic discs, *MNRAS*, 237, 785
- Quinn, P. J., Hernquist, L., & Fullagar, D. P., 1993, Heating of galactic disks by mergers, *ApJ*, 403, 74
- Reshetnikov, V. & Combes, F., 1996, Tidally-triggered disk thickening, I. Observations, *A&AS*, 116, 417
- Reshetnikov, V. & Combes, F., 1997, Tidally-triggered disk thickening, II. Results and interpretations, *A&A*, 324, 80
- Reshetnikov, V. & Combes, F., 1998, Statistics of optical warps, *A&A*, 337, 9
- Revaz, Y. & Pfenniger, D., 2004, Bending instabilities at the origin of persistent warps: A new constraint on dark matter halos *A&A*, 425, 67
- Sanchez-Saavedra, M. L., Battaner, E., & Florido, E., 1990, Frequency of warped spiral galaxies at visible wavelengths, *MNRAS*, 246, 458
- Sancisi, R., 1976, Warped HI disks in galaxies, *A&A*, 53, 159
- Schwarzkopf, U. & Dettmar, R.-J., 2001, Properties of tidally triggered vertical disk perturbations, *A&A373*, 402
- Shaw, M. A. & Gilmore, G., 1990, The luminosity distribution of edge-on spiral and lenticular galaxies. II - Modelling the non-thin disc light in a sample of ten galaxies, *MNRAS*, 242, 59
- Sparke, L., 1995, A bowl-shaped mode of galactic disks, *ApJ*, 439, 42

- Spitzer, L. Jr. & Schwarzschild, M., 1951, The Possible influence of interstellar clouds on stellar velocities, *ApJ*, 114, 385
- Töth, G. & Ostriker, J. P., 1992, Galactic disks, infall, and the global value of Omega, *ApJ*, 389, 5
- van der Kruit, P. C. & Searle, L., 1981a, Surface photometry of edge-on spiral galaxies. I - A model for the three-dimensional distribution of light in galactic disks, *A&A*, 95, 105
- van der Kruit, P. C. & Searle, L., 1981b, Surface Photometry of Edge-On Spiral Galaxies. II - the Distribution of light and color in the disk and spheroid of NGC891, *A&A*, 95, 116
- Waincoat, R. J., Freeman, K. C., & Hyland, A. R., 1989, The optical and near-infrared distribution of light in the edge-on galaxy IC 2531, *ApJ*, 337, 163
- Walker, I. R., Mihos, J. C., & Hernquist, L., 1996, Quantifying the fragility of galactic disks in minor mergers, *ApJ*, 460, 121